

# Dislocation-Mediated Melting in Superfluid Vortex Lattices

S. Andrew Gifford and Gordon Baym

*Department of Physics, University of Illinois at Urbana-Champaign, 1110 West Green Street, Urbana, IL 61801*

(Dated: July 15, 2008)

We describe thermal melting of the two-dimensional vortex lattice in a rotating superfluid by generalizing the Halperin and Nelson theory of dislocation-mediated melting, and derive a melting temperature proportional to the renormalized shear modulus of the vortex lattice. The rigid-body rotation of the superfluid attenuates the effects of lattice compression on the energy of dislocations and hence the melting temperature, while not affecting the shearing. Finally, we discuss dislocations and thermal melting in inhomogeneous rapidly rotating Bose-Einstein condensates; we delineate a phase diagram in the temperature – rotation rate plane, and infer that the thermal melting temperature should lie below the Bose-Einstein transition temperature.

## I. INTRODUCTION

Experiments on rapidly rotating Bose-Einstein condensates (BEC) in harmonic magnetic traps have observed triangular lattices of vortices [1, 2, 3, 4]. The lattice is expected to melt at sufficiently rapid rotation rates,  $\Omega$ , close to the radial trap frequency,  $\omega_\perp$  [5, 6, 7, 8], at sufficiently high energy temperature [9]. In the rapidly rotating regime, the condensate wave function is a linear superposition of single particle states of the lowest Landau level (LLL) in the Coriolis force; quantum fluctuations are predicted [5, 6, 7, 8] to melt the lattice when the number of vortices,  $N_v$ , is so large that the number of particles per vortex (or filling factor),  $\nu$ , falls to  $\sim 6-10$ . While quantum fluctuations increase with decreasing  $\nu$ , thermal fluctuations at finite temperature increase more rapidly. The ratio of the mean square vortex displacements due to thermal fluctuations to those due to quantum fluctuations is  $\sim 10^3 \nu^{-2/3} (T/\Omega) \ln N_v$  [9]. Under typical experimental conditions, melting of the vortex lattice induced by thermal fluctuations is more likely to be observed before melting due to quantum fluctuations.

In this paper, we generalize the Halperin and Nelson (HN) theory of dislocation-mediated melting [10] to apply to the thermal melting of vortex lattices. The HN theory describes thermal melting of lattices as a Kosterlitz-Thouless transition [11] due to unbinding of pairs of elastic dislocations in the lattice. The complication in generalizing the theory is that the forces between vortices in neutral condensates are long ranged, unlike the forces in a crystal lattice. The HN theory has been applied to vortex lattices in type-II superconductors [12], where the forces between vortices are short ranged. It has also been discussed in superfluid helium films [13] under the very limiting assumption that the lattice is incompressible.

We consider a dilute gas of atoms trapped in an external potential and rotating about the z-axis, taking a zero range s-wave interaction between particles with coupling constant,  $g = 4\pi\hbar^2 a_s/m$ , where  $a_s$  is the s-wave scattering length for two bosons; we work in the usual mean field approximation for the interaction energy. Furthermore, we describe the elastic behavior of a vortex lattice

in a rapidly rotating BEC using the coarse-grained, long wavelength elastohydrodynamics description [14]. In lieu of treating the vortices as discrete entities, we express the deviation of the vortices from their equilibrium positions (the triangular lattice sites) as a continuous displacement field,  $\epsilon$ . Although the condensates are three dimensional, the dominant motion is in the rotational plane, to which we confine our attention. The equations of motion couple the local (coarse-grained) velocity field,  $\mathbf{v}$ , the local (coarse-grained) particle density, and the vortex displacement field. In Refs. [7, 9], we used the elastohydrodynamic equations of motion to derive the modes and various correlation functions of system. Here, we use the time-independent form of the same equations to understand the elastic behavior and thermal melting of a superfluid vortex lattice.

Dislocations are expected to form through nonlinear instabilities of vortex lattice excitations, i.e., Tkachenko modes. However, to determine the melting, we need consider only the thermodynamics of dislocations. In doing so, we separate the elastic displacement field into two parts: a fluctuating part from the Tkachenko modes and a singular part from the dislocations. In the absence of nonlinearities these two terms are independent.

Prior to deriving the thermal melting of a superfluid vortex lattice, we first review the elastic equations for a superfluid vortex lattice in Sec. II. Then in Sec. III, we find the elastic displacement field and energy of a single dislocation, and the interaction energy of a dislocation pair. In Sec. IV, we generalize the HN theory of two dimensional melting to a superfluid vortex lattice. Finally, in Sec. V, we consider melting in an inhomogeneous system.

## II. ELASTICITY

In this section we discuss the elastic properties of the vortex lattice, working in the frame in corotating with the lattice. Considering only motion in the transverse plane, we write the energy as a function of the two-dimensional

density  $n$ ,  $\mathbf{v}$  and the vortex displacement field,  $\boldsymbol{\epsilon}$  as [15]

$$E\{n, \mathbf{v}, \boldsymbol{\epsilon}\} = \int \left[ \frac{1}{2} m n v^2 + n V(\mathbf{r}) - \frac{1}{2} m n \Omega^2 r^2 + \frac{1}{2} g_{2d} n^2 + \mathcal{E}_{\text{el}} \right] d^2 r. \quad (1)$$

The first term in Eq. (1) is the kinetic energy of the superfluid surrounding the vortex lattice, in the second  $V(\mathbf{r})$  is the trapping potential, and third term is the centrifugal potential; the fourth term is the interaction energy of the BEC, with  $g_{2d}$  the usual two-dimensional coupling constant ( $\sim Zg$ , where  $Z$  is the axial thickness of the condensate); the final term is the elastic energy density. To second order in  $\boldsymbol{\epsilon}$ ,

$$\mathcal{E}_{\text{el}} = 2C_1(\nabla \cdot \boldsymbol{\epsilon})^2 + C_2 \left[ \left( \frac{\partial \epsilon_x}{\partial x} - \frac{\partial \epsilon_y}{\partial y} \right)^2 + \left( \frac{\partial \epsilon_x}{\partial y} + \frac{\partial \epsilon_y}{\partial x} \right)^2 \right] + \gamma n_v \boldsymbol{\epsilon} \cdot \nabla n. \quad (2)$$

The first two terms in Eq. (2) are the compression and shear energies, respectively, of the vortex lattice;  $C_1$  and  $C_2$  are the (two-dimensional) density-dependent compressional and shear moduli (essentially the usual three dimensional constants [14] integrated over the thickness of the system in the axial direction) [18]. In the incompressible limit, e.g., in liquid helium,  $C_2 = -C_1 = n\hbar\Omega/8$  [14, 16], while in the LLL limit ( $g_{2D}n \ll \hbar\Omega$ ),  $C_2 \approx 0.119g_{2D}n^2$  [6, 17], and  $C_1$  is expected to be small [19]. The final term, in which  $n_v^0 = m\Omega/\pi\hbar$  is the equilibrium vortex density, is the coupling of the vortex displacements to density inhomogeneities, with  $\gamma$  an  $\Omega$ -dependent constant [15]. In the incompressible limit,  $\gamma = (\pi\hbar^2/m) \ln(\ell/\xi_c)$ , where  $\ell = 1/\sqrt{\pi n_v}$  is the vortex (Wigner-Seitz) cell radius,  $\ell^2 = \hbar/m\Omega$ , and  $\xi_c$  is the vortex core radius [15, 20]; in the LLL limit,  $\gamma = \pi\hbar^2/m$  [15].

We first calculate the response of the vortex lattice to a stationary stress to linear order, assuming that the system is effectively two dimensional with motions only in the plane perpendicular to the rotational axis. To linear order, thermal and quantum fluctuations of the vortex positions do not influence the elastic response. The velocity field entering Eq. (1) is governed, in a stationary configuration, by the displacement field of the vortices. Conservation of circulation implies that a shift of the positions of the vortices from their equilibrium positions alters the local velocity of the fluid according to [14]:

$$\mathbf{v} + 2\Omega \times \boldsymbol{\epsilon} = \frac{\hbar}{m} \nabla \Phi, \quad (3)$$

where  $\Phi$  is the non-singular superfluid phase. The curl of this equation,  $(\nabla \times \mathbf{v})_z = -2\Omega \nabla \cdot \boldsymbol{\epsilon}$ , relates the transverse component of the velocity field to the longitudinal component of the displacement field. The steady state velocity field created by a distortion of the vortex lattice

obeys  $\nabla \cdot n\mathbf{v} = 0$ . For a homogeneous system,  $\nabla \cdot \mathbf{v} = 0$ , i.e., the longitudinal component of the velocity vanishes.

Variation of Eq. (1) with respect the particle density and displacement field gives two first order equations of motion,

$$\left( \frac{\delta \mathcal{E}}{\delta n} \right)_{v, \boldsymbol{\epsilon}} = -\gamma n_v^0 \nabla \cdot \boldsymbol{\epsilon} + g_{2D} n = \mu, \quad (4)$$

where  $\mu$  is the chemical potential; and

$$\begin{aligned} \left( \frac{\delta \mathcal{E}}{\delta \boldsymbol{\epsilon}} \right)_{n, v} &= -4\nabla(C_1 \nabla \cdot \boldsymbol{\epsilon}) - 2\nabla \cdot (C_2 \nabla) \boldsymbol{\epsilon} + \gamma n_v^0 \nabla n \\ &\equiv \boldsymbol{\sigma} + \boldsymbol{\zeta}_n, \end{aligned} \quad (5)$$

where  $\boldsymbol{\sigma}$  is the elastic stress [21], and  $\boldsymbol{\zeta}_n = \gamma n_v^0 \nabla n$  is the elastic stress due to density inhomogeneity. (Unlike in [15] we separate out the  $\zeta_n$  term explicitly in defining  $\boldsymbol{\sigma}$ .) In general the elastic constants, dependent on the density, appear within the derivatives. We first consider a homogeneous system, and return to the problem of an inhomogeneous system in Sec. V.

The fluid velocity induced by a displacement of the vortices results in a Coriolis force which balances the elastic and external stresses,  $\boldsymbol{\zeta}$  (including  $\boldsymbol{\zeta}_n$ ):

$$2mn\Omega \times \mathbf{v} = -\boldsymbol{\sigma} - \boldsymbol{\zeta}. \quad (6)$$

The curl and divergence of Eq. (6) yield the transverse and longitudinal elastic responses,  $\epsilon_T$  and  $\epsilon_L$ , independently. Since  $\nabla \cdot n\mathbf{v} = 0$ ,

$$-\sigma_T = 2C_2 \nabla^2 \epsilon_T = \zeta_T, \quad (7)$$

and

$$-\sigma_L - 2mn\Omega v_T = [(4C_1 + 2C_2) \nabla^2 - 4\Omega^2 nm] \epsilon_L = \zeta_L. \quad (8)$$

Fourier transforming Eqs. (7) and (8), we find the elastic Green's functions,  $G_{ij}$  [23],

$$G_{LL}(\mathbf{k}) = \frac{\delta \epsilon_L}{\delta \zeta_L} = -\frac{1}{2(2C_1 + C_2)k^2 + 4\Omega^2 nm}, \quad (9)$$

$$G_{TT}(\mathbf{k}) = \frac{\delta \epsilon_T}{\delta \zeta_T} = -\frac{1}{2C_2 k^2}, \quad (10)$$

and

$$G_{LT}(\mathbf{k}) = G_{TL}(\mathbf{k}) = 0; \quad (11)$$

transverse stresses give rise only to transverse displacements, and longitudinal stresses only to longitudinal displacements. In terms of the elastic Green's functions, the dynamic equations for displacement field are [7],

$$\begin{aligned} i\omega \epsilon_T + \frac{1}{2\Omega mn} G_{LL}^{-1}(\mathbf{k}) \epsilon_L &= \frac{\zeta_L}{2\Omega mn}, \\ i\omega \epsilon_L + \left( \frac{2\Omega \omega^2}{\omega^2 - s^2 k^2} - \frac{1}{2\Omega mn} G_{TT}^{-1}(\mathbf{k}) \right) \epsilon_T &= -\frac{\zeta_T}{2\Omega mn}. \end{aligned} \quad (12)$$

Unlike in conventional elastic systems, the longitudinal elastic Green's function contains an additional length scale, an elastic "penetration depth":

$$\delta^2 = \frac{2C_1 + C_2}{2\Omega^2 mn}. \quad (13)$$

Note that  $C_2 > 0$  while  $C_1$  is generally negative [24], and thus  $\delta^2$  can be positive or negative. In the incompressible regime [25],  $\delta^2 = -\ell^2/16$ , while in the LLL regime,  $\delta^2 \approx 0.03\ell^4/\xi^2 = 0.06(g_{2D}n/\hbar\Omega)\ell^2$ , where  $\xi^2 = \hbar^2/2g_{2D}nm$  is the healing length in the condensate. In the LLL regime,  $\hbar\Omega \gg g_{2D}n$ , and hence in both regimes  $|\delta| \ll \ell$ . Thus within the regime of validity of the coarse-grained continuum approximation,  $G_{LL}(\mathbf{k}) \simeq -1/4\Omega^2 nm$ , and  $G_{LL}(\mathbf{r}, \mathbf{r}') \approx (-1/4\Omega^2 nm)\delta(\mathbf{r} - \mathbf{r}')$ .

The elastic displacement due to the (longitudinal) driving force  $\zeta_n = \gamma n_v^0 \nabla n$  is thus

$$\begin{aligned} \epsilon(\mathbf{r}) &= \int G_{LL}(\mathbf{r}, \mathbf{r}') \zeta_n(\mathbf{r}') d^2 r' \\ &\approx -\frac{\gamma n_v^0}{4\Omega^2 m} \nabla \ln n(\mathbf{r}), \end{aligned} \quad (14)$$

consistent with the results of Refs. [15, 20, 24]. Corrections to this result using the elastic Green's functions for an inhomogeneous system are of order  $1/N_v$ .

### III. DISLOCATIONS

To describe dislocation-mediated melting of a superfluid vortex lattice, we first investigate the structure of

elastic dislocations, which are topological defects in the vortex lattice. Such dislocations obey the condition,

$$\oint d\epsilon = \mathbf{b}, \quad (15)$$

for any closed path around the dislocation, where  $\mathbf{b}$  is the Burger's vector [22, 26]. The minimum length of a Burger's vector is the lattice spacing.

We first solve Eqs. (3) and (6) for an elastic dislocation in a superfluid vortex lattice, leaving mathematical details for the Appendix. For  $\mathbf{b} = b\hat{\mathbf{x}}$  and  $\delta = 0$ , the displacement field is,

$$\begin{aligned} \epsilon_x &= \frac{b}{2\pi} \left[ \tan^{-1}\left(\frac{y}{x}\right) - \frac{xy}{r^2} + \frac{2C_2}{\Omega^2 mn} \frac{xy}{(x^2 + y^2)^2} \right] \\ \epsilon_y &= \frac{b}{2\pi} \left[ \frac{1}{2} \ln(x^2 + y^2) + \frac{x^2}{r^2} + \frac{C_2}{\Omega^2 mn} \frac{y^2 - x^2}{(x^2 + y^2)^2} \right]. \end{aligned} \quad (16)$$

This displacement field is transverse, with vanishing divergence away from the origin, as expected since the longitudinal Green's function vanishes away from the dislocation.

In addition we find that the energy of a single dislocation is

$$E_{\text{dis}} = \frac{C_2 b^2}{\pi} \left[ \ln\left(\frac{R}{a_c}\right) + \frac{4C_2 \delta^2}{2C_1 + C_2} \left[ \frac{1}{a_c^2} \left(1 - \frac{a_c}{2\delta} K_1\left(\frac{a_c}{\delta}\right)\right) - \frac{1}{R^2} \left(1 - \frac{R}{2\delta} K_1\left(\frac{R}{\delta}\right)\right) \right] \right], \quad (17)$$

where  $K_n$  are modified Bessel functions of the second kind, and  $a_c$  is the radius of the dislocation core;  $a_c > a$ , the lattice spacing. We include the dislocation core energy in the chemical potential of the system. In the limit  $R \rightarrow \infty$ , the logarithmic term in Eq. (17) is the

dominant term.

To second order in the displacement field the interactions between dislocations are pairwise. The energy of two separated dislocations at positions  $\mathbf{r}_\alpha$  and  $\mathbf{r}_{\alpha'}$ , with Burger's vectors  $\mathbf{b}_\alpha, \mathbf{b}_{\alpha'}$ , is, as derived in the Appendix,

$$\begin{aligned} E_{\alpha, \alpha'} &= \frac{C_2}{\pi} \left[ \mathbf{b}_\alpha \cdot \mathbf{b}_{\alpha'} \ln\left(\frac{|\mathbf{r}_\alpha - \mathbf{r}_{\alpha'}|}{a_c}\right) - \frac{\mathbf{b}_\alpha \cdot (\mathbf{r}_\alpha - \mathbf{r}_{\alpha'}) \mathbf{b}_{\alpha'} \cdot (\mathbf{r}_\alpha - \mathbf{r}_{\alpha'})}{|\mathbf{r}_\alpha - \mathbf{r}_{\alpha'}|^2} \right. \\ &\quad \left. + \varepsilon_{ij} \varepsilon_{kl} b_{\alpha, i} b_{\alpha', k} \frac{4C_2 \delta^2}{(2C_1 + C_2)} \frac{\partial^2}{\partial x_{\alpha', j} \partial x_{\alpha, l}} \left( \ln|\mathbf{r}_\alpha - \mathbf{r}_{\alpha'}| + K_0\left(\frac{|\mathbf{r}_\alpha - \mathbf{r}_{\alpha'}|}{\delta}\right) \right) \right], \end{aligned} \quad (18)$$

where  $\varepsilon_{ij}$  is the two dimensional anti-symmetric tensor,

The first term in Eq. (18) grows with increasing separa-

tion of the dislocation pairs and is therefore long ranged; the final term decreases with the separation at a rate depending on  $\delta$ . In the limit  $\delta \rightarrow \infty$ , where one recovers classical elasticity, the final term extends to long distances; in this limit, Eq. (18) reduces to the dislocation interaction energy of Ref. [10].

Two dislocations with opposite Burger's vectors are attracted with an interaction which grows logarithmically. Dislocations thus bind in pairs at low temperature. Dislocation-mediated melting is driven, as we discuss in the following section, by unbinding of such pairs.

The core radius,  $a_c$ , the length scale at which the dislocation can no longer be described by a *continuous* displacement field, as well as the dislocation core energy, can only be computed from the local microscopic condensate wave function. In the incompressible limit, the energy of the vortex lattice depends entirely on the kinetic energy of the surrounding superfluid, and thus the core energy is linearly proportional to the density. Similarly, in the rotating frame in the LLL limit, only the interaction energy changes with vortex position, and thus the core energy is proportional to the square of the density. We approximate the dislocation core energy by,

$$E_{\text{core}} \approx a_1 n + a_2 n^2, \quad (19)$$

where  $a_1$  and  $a_2$  are positive functions of the rotation rate, with the approximate dependence,  $a_1 \propto \hbar \Omega a_c^2$  and  $a_2 \propto g a_c^2$ . Since  $E_c$  depends on the position of the vortices within the dislocation core, where the continuum limit is not valid, exact values of  $a_1$  and  $a_2$  must be calculated in terms of the local condensate wave function.

#### IV. DISLOCATION-MEDIATED MELTING

The dislocation-mediated melting of the vortex lattice is a Kosterlitz-Thouless transition [11] arising from unbinding of pairs of elastic dislocations. Thermal fluctuations cause dislocations to enter large systems in pairs with opposite Burger's vectors. Below the melting temperature, pairs are bound; pairs of Burger's vectors of equal magnitude but opposite direction produce no long range elastic deformation, and are thus most stable than isolated dislocations. If two opposite dislocations overlap, they mutually annihilate.

Above the melting temperature, dislocations are unbound, and to a first approximation can be treated independently. In the thermodynamic limit ( $R \rightarrow \infty$ ), the energy (17) is minimized for a dislocation with the minimum magnitude of the Burger's vector, the lattice spacing,  $a$ , and thus  $E_{\text{dis}} \simeq (C_2 a^2 / \pi) \ln(R/a_c)$  plus a small constant. [For a triangular lattice,  $a^2 = (2/\sqrt{3})/n_v$ .] This logarithmic form allows us to apply the simple physical argument of Kosterlitz and Thouless to determine when dislocations are thermodynamically stable in the vortex lattice. Since there are  $\sim (R/a_c)^2$  possible locations for a single dislocation in the vortex lattice, the

entropy of a single dislocation is  $\sim 2 \ln(R/a_c)$ . Hence, the Helmholtz free energy per dislocation is

$$F \approx \left( \frac{C_2 a^2}{\pi} - 2T \right) \ln \left( \frac{R}{a_c} \right). \quad (20)$$

Thus for  $T > C_2 a^2 / 2\pi \equiv T_m^0$ , dislocations (of size  $b = a$ ) are thermodynamically stable. Isolated dislocations remain in the system only above this temperature.

In the absence of interactions between dislocation pairs,  $T_m^0$  would be the melting temperature. As the temperature increases to  $T_m^0$  the mean separation between two dislocations within a pair diverges; in general the mean separation of a pair  $\alpha, \alpha'$  is [11],

$$\langle (\mathbf{r}_\alpha - \mathbf{r}_{\alpha'})^2 \rangle \propto \int e^{-\beta E_{\alpha, \alpha'}(\mathbf{r})} r^2 d^2 r. \quad (21)$$

For  $T < T_m^0$  the mean separation is finite, while for  $T > T_m^0$ , the logarithmic term in Eq. (18) leads to a divergent separation length within a dislocation pair, indicating that the pair has become unbound.

To obtain a more accurate description of melting requires considering interactions of dislocation pairs, which can be taken into account by the renormalization-by-decimation technique in Refs. [27, 28]. This technique requires  $\delta/R$  to be small. We do not give the details here, but note that the net effect is to renormalize the shear modulus  $C_2$  to a temperature dependent function,  $C_{2,R}(T)$ . The shear modulus has an intrinsic dependence on the temperature, since it is proportional to the superfluid density. The melting temperature is then [29]

$$T_m = \frac{a^2}{2\pi} C_{2,R}(T_m). \quad (22)$$

Previous estimates for  $C_{2,R}$  for a lattice of particles interacting logarithmically (e.g., vortices) have shown  $C_{2,R} \approx A C_2$  where  $A \lesssim 1$  [12].

The melting temperature depends only on the shear modulus. It is instructive to compare the origin of this dependence in a system of vortices with the corresponding result in a traditional elastic system (e.g., an isotropic crystal) [10]. The first two terms of Eq. (18) have the same form for the interaction energy of dislocations in an elastic system. The third term of Eq. (18), containing an additional length scale,  $\delta$ , is particular to the vortex system; this term is a short range interaction,  $\sim \delta^2/r^2$ . In smectic liquid crystals near the nematic-to-smectic-A transition, the interaction energy of two dislocations also contains an additional length scale, a penetration depth; when this length is small enough to screen the dislocations in the liquid crystal beyond their core, the dislocation pairs unbind at  $T = 0$  [30]. In such a liquid crystal, *all* the energy channels (splay, twist, and bend) are screened by the compression or stretching of the smectic layers. In the superfluid vortex lattice, however, only compressional effects are screened (by the rigid body motion) while the shearing is unaffected. In the vortex system the unbinding of the dislocations is promoted by shearing alone.

For temperatures approaching  $T_m$  from below, the displacement correlation function is independent of the system parameters [7]:

$$\lim_{T \rightarrow T_m^-} \frac{\langle |\epsilon(\mathbf{r}) - \epsilon(\mathbf{r}')|^2 \rangle}{\ell^2} \approx \frac{1}{2\sqrt{3}\pi} \ln \left( \frac{|\mathbf{r} - \mathbf{r}'|}{\ell} \right). \quad (23)$$

In the solid phase, the vortex lattice exhibits algebraic long-range order. However, above  $T_m$ , the displacement correlations function decay roughly exponentially with distance, as one sees from renormalization group calculations [10].

Extended two dimensional Bose systems, e.g., helium films, or atoms in optical lattices [31, 32, 33], undergo a (conventional) Kosterlitz-Thouless transition [11, 34, 35] to a superfluid state at  $T_{KT} = \pi \hbar^2 n_s / 2m$ , where  $m n_s \equiv \rho_s$  is the two-dimensional superfluid mass density. When rotating at low temperature, such a system should contain a vortex lattice, which melts via a dislocation mediated Kosterlitz-Thouless transition at a temperature  $T_m = a^2 C_{2,R} / 2\pi$ . Using the incompressible shear modulus in  $T_m$  one finds  $T_m / T_{KT} = (1/4\pi\sqrt{3}) n_s(T_m) / n_s(T_{KT})$  [13], where  $n_s(T_m) / n_s(T_{KT}) \approx 1 + b(1 - T_m / T_{KT})^{1/2}$ ;  $b$  in  $^4\text{He}$  films is measured to be  $\simeq 5.5$  [37]. Thus  $T_m / T_{KT} \approx 0.26$ ; renormalization of the shear modulus should reduce this result at most by a factor of 2 [12].

Cozzini et al. find from numerical computation of the  $T = 0$  shear modulus vs.  $\hbar\Omega / g_{2D}n$  – from the incompressible regime ( $\hbar\Omega / g_{2D}n \ll 1$ ) to the LLL regime ( $\hbar\Omega / g_{2D}n \gg 1$ ) – that with the exception of a small increase just above the incompressible regime,  $C_2 \lesssim n\hbar\Omega / 8$  [36]. This result suggests that  $T_m / T_{KT}$  decreases with increasing  $\hbar\Omega / g_{2D}n_s$ . Preliminary calculations for the parameters of the  $^{87}\text{Rb}$  experiment of Ref. [38] give  $b \simeq 4.5$  [39, 40], indicating  $T_m / T_{KT} \lesssim 0.23$  prior to renormalization effects.

## V. MELTING IN AN INHOMOGENEOUS SYSTEM

We expect thermal melting in a rapidly rotating BEC in a finite inhomogeneous geometry also to be driven by formation of dislocations arising from thermal fluctuations. Dislocations have in fact been observed in the lattices in these systems; see Fig. 5a of Ref [1]. However, describing the structure and unbinding of dislocation pairs is much more difficult than in a homogeneous system. On the one hand, the elastic constants,  $C_1$  and  $C_2$ , depend on the local density, and dislocation energies depend on position, while the elastic theory contains second order terms explicitly dependent on  $\epsilon$  in addition to the usual terms dependent on derivatives of  $\epsilon$  [19]. Furthermore, in a finite system dislocations can be created not only in pairs in the bulk of the system, but an isolated dislocation can also be formed at the edge, which separates from its image dislocation and moves into the bulk. Such additional features must be taken into account numerically

to determine the details of melting, a problem we leave for the future [41].

Here we simply determine an upper bound on the melting temperature. We assume that the maximum density,  $n_0$ , of the BEC occurs at the center of the trap, where a dislocation has maximum energy. Furthermore, this maximum energy is less than the energy of a dislocation in a condensate of the same size but with uniform density,  $n_0$ . As a dislocation approaches the edge of the trap, its energy goes to zero. Thus the dislocation energy in an inhomogeneous system is bounded above by

$$E_{\text{dis}}(\mathbf{r}) \leq \max\{E_{\text{dis}}\} < (C_2(0)a^2/\pi) \ln(R_{\text{TF}}/a_c), \quad (24)$$

where  $C_2(0)$  is the (unrenormalized) shear modulus at the center of the trap, and  $R_{\text{TF}}$  is the Thomas-Fermi radius of the rotating cloud. Using an upper bound to the dislocation energy should yield an upper bound on the melting temperature, and thus Eq. (20) indicates that the temperature at which dislocations are thermodynamically stable is bounded above by  $T_m^0 = C_2(0)a^2/2\pi$ . In fact, dislocations should appear near the edge of the BEC for temperatures below  $T_m^0$  and creep towards the center as the  $T$  approaches  $T_m^0$ , while for  $T \gtrsim T_m^0$ , we expect dislocations to occur throughout the system.

Melting generally occurs below the Bose-Einstein condensation temperature,  $T_c \approx 0.94\hbar(N\omega_z(\omega_\perp^2 - \Omega^2))^{1/3}$ , where  $\omega_z$  and  $\omega_\perp$  are the azimuthal and radial angular frequencies of the trap respectively. We first estimate  $T_m^0/T_c$  in the limit of a nearly incompressible fluid ( $\hbar\Omega \ll gn$ ) in trap geometry, and then consider the LLL limit. In the former regime,  $T_m^0 = C_2(0)a^2/2\pi \lesssim \hbar\Omega n_s(0)a^2/16\pi = \rho_s(0)\hbar^2/8\sqrt{3}m^2$ , where  $\rho_s(0)$  the (two dimensional) superfluid mass density at the center of the trap. The shear modulus depends on the superfluid mass density a function of temperature, which for a weakly interacting Bose gas is approximately the product of the mass, the mean thickness, and the three dimensional condensate density,  $n_{\text{TF}}(r=0, T)$ . At the center of the trap the condensate density, coarse-grained over the vortices, is approximately homogeneous and does not feel the effect of the condensate edge; at  $T = 0$ ,

$$n_{\text{TF}}(r=0, T=0) = \frac{\hbar\omega_\perp}{2gb_\Delta} \left[ \frac{15Nb_\Delta a_s}{d_\perp} \frac{\omega_z}{\omega_\perp} \left( 1 - \frac{\Omega^2}{\omega_\perp^2} \right) \right]^{\frac{2}{5}}. \quad (25)$$

In writing Eq. (25), we approximate the number of particles in the condensate by the total particle number  $N$ ;  $d_\perp = \hbar/\sqrt{m\omega_\perp}$  is the radial trap length, and  $b_\Delta \approx 1.1596$  is the Abrikosov parameter [42]. At finite temperature,  $n_{\text{TF}}(r=0, T) = n_{\text{TF}}(r=0, 0)(1 - (T/T_c)^{3/2})$ . The thickness,  $Z$ , of the condensate at the center of the trap is approximately  $d_z(2gb_\Delta n_{\text{TF}}(0)/\hbar\omega_z)^{1/2}$ , where  $d_z = \hbar/\sqrt{m\omega_z}$  is the azimuthal trap length.

Thus we find  $T_m/T_c$  as the solution of

$$\frac{T_m}{T_c} \lesssim 0.0049 N^{4/15} \left( \frac{d_z}{b_\Delta a_s} \right)^{2/5} \left( \frac{d_z}{d_\perp} \right)^{16/15} \left( 1 - \frac{\Omega^2}{\omega_\perp^2} \right)^{4/15} \left( 1 - \left( \frac{T_m}{T_c} \right)^{\frac{3}{2}} \right). \quad (26)$$

For the experimental parameters of Refs. [2, 3] in  $^{87}\text{Rb}$  ( $a_s = 4.8 \pm 0.05$  nm,  $d_\perp = 3.75$   $\mu\text{m}$ ,  $d_z = 4.69$   $\mu\text{m}$ ) with  $10^4$  particles and  $\Omega = 0.9\omega_\perp$ , we have  $T_m/T_c \lesssim 0.49$ . For  $N = 10^6$  this ratio increases to  $T_m/T_c \lesssim 0.78$ . If  $T_m/T_c$  is only slightly less than unity, then the thermal melting of the vortex lattice will be hard to observe experimentally. Higher rotation rates help to lower the melting temperature, but in most experiments, the number particles in the system decreases too, making thermal melting harder to resolve. Note that Eq. (26) predicts that  $T_m/T_c$  decreases with increasing scattering length, allowing for the possibility of inducing thermal melting via a Feshbach resonance.

In the LLL limit, the density at the center of the trap is [43],

$$n_{\text{LLL}}(r=0, T=0) = \frac{1}{2\pi^{5/4}} \left( \frac{N}{b_\Delta d_\perp^4 d_z a_s} \left( 1 - \frac{\Omega^2}{\omega_\perp^2} \right) \right)^{\frac{1}{2}}. \quad (27)$$

Along the axis, the condensate particles are in the lowest harmonic oscillator state, so the thickness of the condensate at the center of the trap is approximately  $d_z$ . Also at the center of the trap, the condensate is in a harmonic oscillator state along the axis and approximately homogeneous in the plane of rotation, so the density as a function of temperature is proportional to  $1 - (T/T_c)^2$ , which we take as the temperature dependence of  $C_2$  in the LLL regime. The melting temperature is given by the solution of

$$\frac{T_m}{T_c} \approx 0.0036 \left( \frac{N d_z}{d_\perp} \right)^{2/3} \frac{\omega_\perp}{\Omega} \left( 1 - \frac{\Omega^2}{\omega_\perp^2} \right)^{2/3} \left( 1 - \left( \frac{T_m}{T_c} \right)^2 \right). \quad (28)$$

Figure 1 shows schematically the phase diagram of a rapidly rotating BEC. The y-axis is the temperature divided by the condensation temperature, and the x-axis is the “rotational rapidity,”  $y = \tanh^{-1}(\Omega/\omega_\perp)$  [43]. In this figure we use the parameters of Refs. [2, 3] as above. The curve separating the vortex lattice and vortex liquid phases is given by Eq. (26) at low rotation, (28) at high rotation rates, and an interpolation between the two limits; the two kinks in the curve are artifacts of using these two limits with the interpolation. We assume that the melting leads directly to a vortex liquid, neglecting a possible hexatic phase intermediate between the vortex lattice and liquid which exhibits no long-range order of the vortex positions but maintains algebraic long-range order of the triangular orientation of the lattice [10]. Computing the phase boundary between such a hexatic phase and a vortex liquid requires microscopic details of the dislocations (e.g., core radius and energy) beyond the scope of this paper.

The vortex lattice is predicted to melt via quantum fluctuations into a new strongly correlated regime. Details of this regime are discussed in Refs. [5, 6, 44]. With

the density Eq. (27) and  $\nu \approx n/n_v$ , we estimate the phase boundary for the strongly correlated system to be at

$$\frac{\Omega_c}{\omega_\perp} \approx \left[ 1 + \left( \frac{4\sqrt{\pi} b_\Delta a_s}{N d_z} \right) \nu_c^2 \right]^{-\frac{1}{2}}. \quad (29)$$

In Fig. 1, where we take a critical filling fraction,  $\nu_c \sim 10$  [6, 7], the phase boundary is indicated by the vertical dotted line, at  $y \simeq 5.4$  (corresponding to  $\Omega/\omega_\perp \approx 0.99996$ ). The phase diagram remains to be studied in detail, e.g., near the region where the vortex liquid phase boundary intercepts the strongly correlated regime, and the behavior at higher temperatures.

At low rotation rates ( $\Omega/\omega_\perp \simeq 0.9$ ), the melting temperature may be too close to the condensation temperature to discern the melting of the vortex lattice experimentally. Higher rotation rates provide a better opportunity to observe melting since  $T_m$  decreases with  $\Omega/\omega_\perp$ . However, at sufficiently high rotation rates (e.g., at  $y \sim 5$  in Fig. 1), it is not clear how to experimentally distinguish thermal melting from quantum melting, since we do not have an adequate understanding of the melted

states at finite temperature.

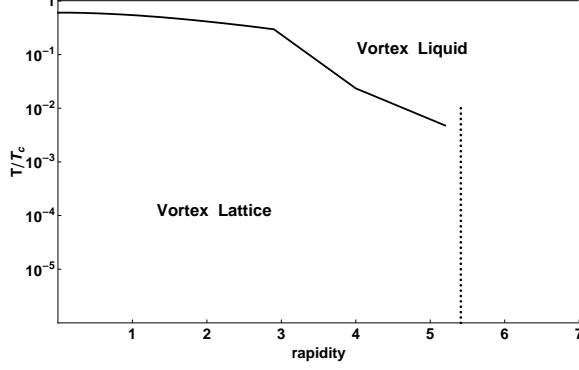


FIG. 1: Sketch of the phase diagram of rapidly rotating BEC. The temperature is in units of the condensation temperature,  $T_c$ ; the “rotational rapidity” is defined as  $y = \tanh^{-1}(\Omega/\omega_\perp)$  [43]. To the right of the dotted line, the system at lower temperatures enters a strongly correlated regime.

## VI. CONCLUSION

The elasticity of a superfluid vortex lattice is determined by the energy of the vortex cells and the global rotational fluid flow; the kinetic energy of the “rigid-body” rotational velocity stabilizes the system against a negative compression modulus,  $C_1$ . Because of the rotational motion, the effect of elastic compression is significantly weakened, and shearing is the dominant degree of freedom for the vortex lattice. Correspondingly, we find that the melting temperature of the vortex lattice depends only on the (renormalized) shear modulus.

Among the unanswered questions for future examination are, first, to delineate the properties of the dislocation core, which will require extensive computation to unveil. Dislocation cores play a significant role in finite sized systems; in experiments to date, core radii may be only an order of magnitude smaller than the system size. Also, one needs to take into account a possible transition to a hexatic phase, and then the transition of the hexatic to a vortex liquid. The latter process involves the unbinding of the dislocations into disclination pairs, whose description requires the energy and size of the dislocation core [10].

Dislocations in non-uniform condensates present further unsolved problems, analogous to those for vortices in inhomogeneous systems, for example, the dependence

of the energy of a dislocation on position. This dependence is needed to determine whether it is energetically preferable for dislocations to form at the edge, or by unbinding in the bulk of the condensate.

We thank Markus Holzmann for helpful discussions and Joshua Rubin. This work was supported in part by NSF Grants PHY03-55014, PHY05-00914, and PHY07-01611.

## APPENDIX

In this Appendix we derive the velocity and displacement fields around an elastic dislocation in a homogeneous two-dimensional vortex lattice, in particular, for superfluid vortex lattices, a two-dimensional edge dislocation [26]. The challenge is to find a solution of Eqs. (3) and (6) that satisfies Eq. (15) for the Burger’s vector. We first recast Eq. (15) as

$$\varepsilon_{ij} \frac{\partial w_{jk}}{\partial x_i} = b_k \delta(\mathbf{r} - \mathbf{r}'), \quad (30)$$

where  $\varepsilon_{ij}$  is the anti-symmetric tensor, and  $w_{ij} = \partial \epsilon_j / \partial x_i$ . Note that  $\epsilon$  is not continuous within the entire plane (i.e.,  $\partial^2 \epsilon / \partial x \partial y \neq \partial^2 \epsilon / \partial y \partial x$ ); otherwise, Eq. (30) is not valid.

To satisfy the conditions,  $\nabla \cdot \mathbf{v} = 0$  and  $\boldsymbol{\sigma} + 2mn\boldsymbol{\Omega} \times \mathbf{v} = 0$ , we define two dual (gauge) fields, the stream function,  $\psi$ , and a modified Airy stress function,  $\chi$ . Using the elastic stress tensor,  $\sigma_{ij}$ , defined from Eq. (5) such that  $\sigma_j = -\partial \sigma_{ij} / \partial x_i$ , we write,

$$v_i = \varepsilon_{ij} \frac{\partial \psi}{\partial x_j} \quad (31)$$

$$\sigma_{ij} = \varepsilon_{ik} \varepsilon_{jl} \frac{\partial^2 \chi}{\partial x_k \partial x_l} - 2mn\Omega \delta_{ij} \psi. \quad (32)$$

Substituting these expressions into the curl of Eq. (3) and Eq. (30), we have,

$$\frac{2C_1 + C_2}{16C_1C_2} \nabla^4 \chi - \frac{mn\Omega}{4C_1} \nabla^2 \psi = (\nabla \times \mathbf{b} \delta(\mathbf{r} - \mathbf{r}'))_z \quad (33)$$

$$\frac{\Omega}{4C_1} \nabla^2 \chi + \nabla^2 \psi - \frac{mn\Omega^2}{C_1} \psi = 0, \quad (34)$$

where  $\mathbf{r}'$  is the position of the dislocation. Taking  $\mathbf{r}' = 0$ , we find

$$\chi(\mathbf{r}) = \varepsilon_{ij} b_j \frac{\partial}{\partial x_i} \left[ \frac{C_2}{\pi} |\mathbf{r}|^2 \left( \ln \left( \frac{|\mathbf{r}|}{a} \right) - 1 \right) + \frac{4C_2^2 \delta^2}{(2C_1 + C_2)\pi} \left( \ln |\mathbf{r}| + K_0 \left( \frac{|\mathbf{r}|}{\delta} \right) \right) \right] \quad (35)$$

$$\psi(\mathbf{r}) = \varepsilon_{ij} b_j \frac{\partial}{\partial x_i} \left[ \frac{2C_2 \Omega \delta^2}{(2C_1 + C_2)\pi} \left( \ln |\mathbf{r}| + K_0 \left( \frac{|\mathbf{r}|}{\delta} \right) \right) \right]. \quad (36)$$

The Airy stress function contains two basic terms. For finite  $\delta$ , the first term in Eq. (35) is long ranged while the second term dies off. The stream function is proportional to this second term. For imaginary  $\delta$  we replace  $K_0(x)$  by  $-\frac{\pi}{2}Y_0(x)$  (where  $Y_0$  is a modified Bessel function of the first kind) since  $\chi(\mathbf{r})$  and  $\psi(\mathbf{r})$  are real. [For  $\delta \rightarrow \infty$ , we find the typical results for an edge dislocation in two dimensions (see Ref [22]), however, this limit is not physically relevant here.]

### A. Energy of a Single Dislocation

According to Eq. (15), the displacement field,  $\epsilon$ , along any closed path around a dislocation does not return to its initial value. Instead, the displacement field at the close of the loop is equal to its initial value plus the Burger's vector. Thus, the system includes a "branch cut" from the dislocation core to the edge of the system, as in Fig. 2; the displacement field for a dislocation is single valued. (This structure is similar to that of the phase,  $\phi$ , around a vortex, which changes from 0 to  $2\pi$ ; jumping by  $2\pi$  across the branch cut.)

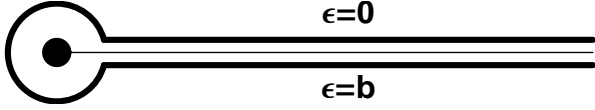


FIG. 2: Branch cut extending from the core of a dislocation.

The energy of an elastic displacement in the superfluid vortex lattice is,

$$E_{\text{el}} = \int \left[ 2C_1 (\nabla \cdot \epsilon)^2 + \frac{1}{2} nm |\mathbf{v}_T|^2 + C_2 \left[ \left( \frac{\partial \epsilon_x}{\partial x} - \frac{\partial \epsilon_y}{\partial y} \right)^2 + \left( \frac{\partial \epsilon_x}{\partial y} + \frac{\partial \epsilon_y}{\partial x} \right)^2 \right] \right] d^2 r, \quad (37)$$

where  $\mathbf{v}_T$  is the transverse flow velocity. Integrating by parts and using  $|\mathbf{v}_T|^2 = 2\epsilon \cdot \Omega \times \mathbf{v}$ , from Eq. (3), we have

$$E_{\text{el}} = \oint \left[ 2C_1 \frac{\partial \epsilon_i}{\partial x_i} \epsilon_j + C_2 \left( \left( \frac{\partial \epsilon_i}{\partial x_j} + \frac{\partial \epsilon_j}{\partial x_i} \right) \epsilon_i - (\nabla \cdot \epsilon) \epsilon_j \right) \right] d\Sigma_j \quad (38)$$

+  $\int \epsilon \cdot [-2C_1 \nabla (\nabla \cdot \epsilon) - C_2 \nabla^2 \epsilon + nm \Omega \times \mathbf{v}] d^2 r$ , where  $\Sigma_j$  is the normal component of the surface element of the section of the boundary (including the branch cut). In the absence of external forces, Eq. (6) implies that the integrand in the second integral in Eq. (38) is zero. The integrals at the boundary of the system and around the core are negligible; the branch cut contribution is dominant. Since  $\epsilon = \mathbf{b}$  on the lower part of the branch cut, and  $\epsilon = 0$  on the upper part (Fig. 2), we find finally

$$E_{\text{el}} = \int [2C_1 b_j (\nabla \cdot \epsilon) + C_2 \left( b_i \frac{\partial \epsilon_i}{\partial x_j} + b_i \frac{\partial \epsilon_j}{\partial x_i} - b_j (\nabla \cdot \epsilon) \right)] d\Sigma_j^-, \quad (39)$$

where the integral is along the lower branch. Computing this expression using Eqs. (31) and (32), relating the derivatives of  $\epsilon$  to  $\sigma_{ij}$  [21], and (35) and (36), we obtain Eq. (17).

### B. Energy of Many Interacting Dislocations

To obtain a more realistic description of the system, requires taking into account the interactions of dislocations. To compute the energy of a two-dimensional gas of interacting dislocations we first substitute Eq. (31) and Eq. (32) into Eq. (37) by relating the derivatives of  $\epsilon$  to  $\sigma_{ij}$  [21], and find,

$$E_{\text{el}} = \int \left[ \frac{1}{8C_2} \left( \frac{\partial^2 \chi}{\partial x_i \partial x_j} \right)^2 - \frac{2C_1 - C_2}{32C_1 C_2} (\nabla^2 \chi)^2 - \frac{mn\Omega}{4C_1} \psi \nabla^2 \chi + \frac{(mn\Omega)^2}{2C_1} \psi^2 + \frac{1}{2} mn |\nabla \psi|^2 \right] d^2 r. \quad (40)$$

We consider an aggregate of dislocations with Burger's vectors,  $\mathbf{b}_\alpha(\mathbf{r}_\alpha)$ , such that the sum over all Burger's vectors is zero and  $\chi(\mathbf{r})$  and its derivatives are zero at infinity – unlike a single dislocation, a pair of dislocations with equal and opposite Burger's vectors is not long ranged. Integrating Eq. (41) by parts we obtain,

$$E_{\text{el}} = \frac{1}{2} \int \chi \left( \frac{2C_1 + C_2}{16C_1 C_2} \nabla^4 \chi - \frac{mn\Omega}{4C_1} \nabla^2 \psi \right) d^2 r, \quad (41)$$

and substituting in Eq. (33) and Eq. (35), and integrating, we derive Eq. (18).

[1] J.R. Abo-Shaeer, C. Raman, J.M. Vogels, and W. Ketterle, Science **292**, 476 (2001).

[2] I. Coddington, P. Engels, V. Schweikhard, and E.A. Cor-



- nell, Phys. Rev. Lett. **91**, 100402 (2003).
- [3] V. Schweikhard, I. Coddington, P. Engels, V.P. Mogen-  
dorff, and E.A. Cornell, Phys. Rev. Lett. **92**, 040404  
(2004).
- [4] V. Bretin, S. Stock, Y. Seurin, and J. Dalibard, Phys.  
Rev. Lett. **92**, 050403 (2004).
- [5] N.R. Cooper, N.K. Wilkin and J.M.F. Gunn, Phys. Rev.  
Lett. **87**, 120405 (2001).
- [6] J. Sinova, C.B. Hanna, and A.H. MacDonald, Phys. Rev.  
Lett. **89**, 030403 (2002).
- [7] G. Baym, Phys. Rev. A **69**, 043618 (2004).
- [8] T.K. Ghosh and G. Baskaran, Phys. Rev. A **69** 023603  
(2004).
- [9] S.A. Gifford and G. Baym, Phys. Rev. A **70**, 033602  
(2004).
- [10] B.I. Halperin and D.R. Nelson, Phys. Rev. Lett. **41**, 121  
(1978); **41**, 519(E) (1978); and D.R. Nelson and B.I.  
Halperin, Phys. Rev. B **19**, 2457 (1979).
- [11] J.M. Kosterlitz and D.J. Thouless, J. Phys. C **6**, 1181  
(1973).
- [12] D.S. Fisher, Phys. Rev. B **22**, 1190 (1980).
- [13] B.A. Huberman and S. Doniach, Phys. Rev. Lett. **43**,  
950 (1979).
- [14] G. Baym and E. Chandler, J. Low Temp. Phys. **50**, 57  
(1983); E. Chandler and G. Baym, J. Low Temp. Phys.  
**62**, 119 (1986).
- [15] G. Baym, C.J. Pethick, S.A. Gifford, and G. Watanabe,  
Phys. Rev. A **75**, 013602 (2007).
- [16] V.K. Tkachenko, Zh. Esp. Teor. Fiz. **49**, 1875 (1965)  
[Sov. Phys. JETP **22**, 1282 (1966)]; Zh. Esp. Teor. Fiz.  
**50**, 1573 (1966) [Sov. Phys. JETP **23**, 1049 (1966)]; Zh.  
Esp. Teor. Fiz. **56**, 1763 (1969) [Sov. Phys. JETP **29**,  
245 (1969)].
- [17] E.B. Sonin, Phys. Rev. A, **72**, 021606(R) (2005).
- [18] The Lamé coefficients,  $\mu$  and  $\lambda$ , used in [10], are related  
to the moduli  $C_1$  and  $C_2$  in two dimensions by  $\mu = 2C_2$   
and  $\mu + \lambda = 4C_1$ .
- [19] G. Watanabe, G. Baym and C. J. Pethick, to be pub-  
lished.
- [20] D. E. Sheehy and L. Radzihovsky, Phys. Rev. A **70**,  
051602(R) (2004).
- [21] The elastic stress force,  $\sigma$ , is related to the usual elastic  
stress tensor,  $\sigma_{ij} = 4C_2 u_{ij} + (4C_1 - 2C_2) u_{kk} \delta_{ij}$ , by  $\sigma_i =$   
 $\partial \sigma_{ij} / \partial x_j$ , where  $u_{ij} = (\partial \epsilon_i / \partial x_j + \partial \epsilon_j / \partial x_i) / 2$  [22].
- [22] L.D. Landau and E.M. Lifshitz, *Theory of Elasticity*  
(Butterworth-Heinemann, Oxford, 2006).
- [23] Since  $2C_1 + C_2 \leq 0$  in (and near) the incompressible limit,  
 $G_{LL}$  changes sign for  $k^2 \geq -2\Omega^2 nm / (2C_1 + C_2) \simeq 16/\ell^2$ ,  
which according to Eq. (12) should be accompanied by a  
resonant  $\omega^2$  becoming negative. This change of sign does  
not imply an instability of the lattice, since it occurs  
for wavelengths  $\lesssim$  the vortex lattice spacing, a length  
scale at which the elastohydrodynamic description is no  
longer valid. In general, a conventional elastic system is  
unstable if  $C_1 < 0$  [22]; however, in the vortex case the  
kinetic energy term in Eq. (1) guarantees the stability of  
the lattice.
- [24] G. Watanabe, G. Baym and C. J. Pethick, Phys. Rev.  
Lett. **93**, 190401 (2004).
- [25] For  $\delta^2 > 0$ , the elastic Green's function of the vortex  
lattice decays exponentially, while, if  $\delta^2 < 0$ , then the  
penetration depth is imaginary, suggesting ripples in the  
displacement field. In the regime where  $\delta^2$  is negative, the  
quasi-wavelengths of any undulations in the displacement  
are  $\lesssim \ell/4$ .
- [26] F. R. N. Nabarro, *Theory of Crystal Dislocations* (Claren-  
don, Oxford, 1967).
- [27] A.P. Young, Phys. Rev. B **19**, 1855 (1979).
- [28] J.M. Kosterlitz, J. Phys. C **7**, 1046 (1974).
- [29] The dependence of  $T_m$  on  $\delta$  is negligible in the region  
 $\delta \lesssim a_c$ . If one assumes incompressibility,  $C_{1,R} \rightarrow \infty$ , as  
in the derivation of  $T_m$  in Ref. [13], for which  $\delta$  becomes  
effectively infinite, the melting temperature is given by  
the limit of  $(a^2/\pi)C_{1,R}C_{2,R}/(2C_{1,R} + C_{2,R})$ , where the  
 $C$ 's are the renormalized elastic moduli. However, this  
limit is unphysical, since the Tkachenko mode frequencies  
are finite only if  $C_{1,R}$  is finite.
- [30] A.R. Day, T.C. Lubensky and A.J. McKane, Phys. Rev.  
A **27**, 1461 (1983).
- [31] S. Stock, Z. Hadzibabic, B. Battelier, M. Cheneau, and  
J. Dalibard, Phys. Rev. Lett. **95**, 190403 (2005).
- [32] V. Schweikhard, S. Tung, and E. A. Cornell, Phys. Rev.  
Lett. **99**, 030401 (2007).
- [33] M. Holzmann, G. Baym, J.P. Blaizot, and F. Laloe,  
PNAS **104**, 1476 (2007).
- [34] V.L. Berezinskii, Sov. Phys. JETP **32**, 493 (1971); **34**,  
610 (1972).
- [35] D.R. Nelson and J.M. Kosterlitz, Phys. Rev. Lett. **39**,  
1201 (1977).
- [36] M. Cozzini, S. Stringari, and C. Tozzo, Phys. Rev. A **73**,  
023615 (2006).
- [37] D.J. Bishop and J.D. Reppy, Phys. Rev. B **22**, 5171  
(1980).
- [38] Z. Hadzibabic, P. Krüger, M. Cheneau, S. Rath, and J.  
Dalibard, New J. Phys., **10**, 045006 (2008).
- [39] M. Holzmann (private communication).
- [40] M. Holzmann and W. Krauth, Phys. Rev. Lett. **100**,  
190402 (2008).
- [41] In Sec. II, we separated out the elastic force due to an in-  
homogeneous density,  $\zeta_n = \gamma n_v^0 \nabla n$ , and treated it as an  
external stress. This force only affects the displacement  
field of the vortex lattice, according to Eq. (14), and does  
not influence the displacement field of the dislocation.  
However, the coupling between the particle density and  
the vortex density contributes a term to the dislocation  
energy,
- $$\Delta E = \int \gamma n(\mathbf{r}) \delta n_v d^2 r = - \int \gamma n(\mathbf{r}) n_v^0 \nabla \cdot \epsilon d^2 r.$$
- Using Eqs. (3), (31), and (36), we find for a vortex at  $\mathbf{r}_0$ ,
- $$\Delta E = \alpha \int n(\mathbf{r}) \frac{\mathbf{b} \times (\mathbf{r} - \mathbf{r}_0)}{|\mathbf{r} - \mathbf{r}_0|^2} K_1 \left( \frac{|\mathbf{r} - \mathbf{r}_0|}{\delta} \right) d^2 r, \quad (42)$$
- where  $\alpha = \gamma C_2 n_v^0 / (2C_1 + C_2) \pi$ . But because  $\delta < \ell$ , this  
term is small and does not contribute significantly to the  
overall energy.
- [42] U.R. Fischer and G. Baym, Phys. Rev. Lett. **90**, 140402  
(2003).
- [43] G. Baym and C.J. Pethick, Phys. Rev. A **69**, 043619  
(2004).
- [44] G. Baym, J Low Temp. Phys. **138**, 601 (2005).